◆ Human Brain Mapping 36:1524–1535 (2015) ◆

Sex Differences in Normal Age Trajectories of Functional Brain Networks

Dustin Scheinost,[1]* Emily S. Finn,[2] Fuyuze Tokoglu,[1] Xilin Shen,[1] Xenophon Papademetris,[1,3] Michelle Hampson,[1] and R. Todd Constable[1,2,4]

[1]*Department of Diagnostic Radiology, Yale School of Medicine, New Haven, Connecticut*
[2]*Interdepartmental Neuroscience Program, Yale University, New Haven, Connecticut*
[3]*Department of Biomedical Engineering, Yale University, New Haven, Connecticut*
[4]*Department of Neurosurgery, Yale School of Medicine, New Haven, Connecticut*

Abstract: Resting-state functional magnetic resonance image (rs-fMRI) is increasingly used to study functional brain networks. Nevertheless, variability in these networks due to factors such as sex and aging is not fully understood. This study explored sex differences in normal age trajectories of resting-state networks (RSNs) using a novel voxel-wise measure of functional connectivity, the intrinsic connectivity distribution (ICD). Males and females showed differential patterns of changing connectivity in large-scale RSNs during normal aging from early adulthood to late middle-age. In some networks, such as the default-mode network, males and females both showed decreases in connectivity with age, albeit at different rates. In other networks, such as the fronto-parietal network, males and females showed divergent connectivity trajectories with age. Main effects of sex and age were found in many of the same regions showing sex-related differences in aging. Finally, these sex differences in aging trajectories were robust to choice of preprocessing strategy, such as global signal regression. Our findings resolve some discrepancies in the literature, especially with respect to the trajectory of connectivity in the default mode, which can be explained by our observed interactions between sex and aging. Overall, results indicate that RSNs show different aging trajectories for males and females. Characterizing effects of sex and age on RSNs are critical first steps in understanding the functional organization of the human brain. *Hum Brain Mapp 36:1524–1535, 2015.*

Key words: sex differences; aging; resting state; brain networks; functional connectivity

INTRODUCTION

The functional organization of neural systems distributed across the brain may provide key insights into normal cognition and neurological and psychiatric disorders. Resting-state functional magnetic resonance imaging (rs-fMRI) is increasingly used to study human brain organization, as spatiotemporal patterns of brain activity at rest cluster into distinct sets of resting-state networks (RSNs; Damoiseaux et al., 2006). RSNs divide the brain along boundaries that are roughly consistent with known functional areas (Smith et al., 2009) and have been linked with cognitive functions (Cole et al., 2012; Hampson et al., 2006). A subset of RSNs including the default-mode network (DMN), the fronto-parietal network (FPN), and

Contract grant sponsor: NIH; Contract grant number: T32 DA022975

*Correspondence to: Dustin Scheinost, Department of Diagnostic Radiology, Yale School of Medicine, 300 Cedar Street, PO Box 208043, New Haven, CT 06520-8043, USA. E-mail: dustin.scheinost@yale.edu

Received for publication 12 October 2014; Revised 27 November 2014; Accepted 4 December 2014.

DOI: 10.1002/hbm.22720

Published online 18 December 2014 in Wiley Online Library (wileyonlinelibrary.com).

sensory (e.g., auditory and visual) networks have been consistently reported in the literature (Damoiseaux et al., 2006; Smith et al., 2009; Yeo et al., 2011). Changes in connectivity strength of many of these networks, for example the DMN, have received considerable research attention as markers of neurocognitive disorders such as Alzheimer's diease (Buckner et al., 2008; Damoiseaux, 2012). Nevertheless, basic properties of these networks such as the effects of sex and aging are not fully understood. Characterizing any sex differences in the aging trajectories of RSNs remain critical steps in differentiating normal development from pathological changes.

In adulthood, many sex differences in brain structures and functions exist (Cosgrove et al., 2007) and, likewise, sex differences in RSNs have been reported. Nevertheless, the locations of these differences vary across studies. Sex differences in the DMN are the most commonly reported as females generally displaying greater connectivity (Allen et al., 2011; Biswal et al., 2010; Bluhm et al., 2008; Filippi et al., 2013; Tomasi and Volkow, 2012b), although it has also been reported that peripheral nodes of the DMN exhibit greater connectivity in males over females (Allen et al., 2011; Filippi et al., 2013). Some studies report that sensory networks such as the visual networks have greater connectivity in males (Biswal et al., 2010; Filippi et al., 2013); however, these differences are not always found (Allen et al., 2011; Tomasi and Volkow, 2012b). Studies of attention networks show conflicting results: some report that connectivity is higher in males (Allen et al., 2011; Bluhm et al., 2008), while others report that connectivity is higher in females (Allen et al., 2011; Filippi et al., 2013). Finally, some studies have failed to observe any sex differences in RSNs (Weissman-Fogel et al., 2010), suggesting that a complete picture of sex differences in the adult brain is not fully developed.

RSNs are plastic throughout the lifespan. Maturation from childhood to adulthood is marked by a shift from local to distributed networks (Fair et al., 2009) with the strength of long-range connections peaking in late adolescence and early adulthood. Connectivity in RSNs such as the DMN and the FPN eventually decreases through adulthood (Allen et al., 2011; Hampson et al., 2012) with sharper deceases in the elderly (Andrews-Hanna et al., 2007). Older adults also show decreased modularity and decreased local efficiency in these networks compared to younger adults (Geerligs et al., in press). Although connectivity mainly decreases throughout adulthood, sensory networks (Biswal et al., 2010; Geerligs et al., in press) and subcortical regions (Hampson et al., 2012) may increase connectivity with aging during adulthood.

While sex and aging effects are observed in RSNs, these variables are often investigated independently (Geerligs et al., in press). Studies have used a limited age range (Filippi et al., 2013) or well-matched age distributions to minimize effects of age when investigating sex differences (Bluhm et al., 2008; Weissman-Fogel et al., 2010), which makes it difficult to ascertain the expected sex difference across the age range for RSNs. When both effects are studied together, inconsistent interactions have been reported (Allen et al., 2011; Zuo et al., 2010). If RSNs in males and females age differently, it may explain some inconsistencies in previously reported sex differences, and suggest that effects of both demographic variables are important to characterize normal changes over the lifespan.

Here, we investigated sex differences in aging trajectories for RSNs using a voxelwise graph-theoretic measure, the intrinsic connectivity distribution (ICD; Scheinost et al., 2012). ICD examines each voxel's connectivity to every other voxel in the brain and enables characterization of specific voxel's full range of connectivity. Many previous studies of sex differences have primarily relied on independent component analysis (ICA) (Allen et al., 2011; Biswal et al., 2010; Bluhm et al., 2008; Filippi et al., 2013; Weissman-Fogel et al., 2010). As group ICA estimates a common set of components or networks for the whole group, subtle differences between participants, such as sex difference in aging trajectories, may be lost (Svensén et al., 2002). In contrast to ICA, voxelwise connectivity methods such as ICD do not constrain voxels to particular networks and may provide greater sensitivity to subtle differences. In a sample of males and females ranging from early adulthood to late middle age, we hypothesized that our exploratory analysis would reveal sex and aging effects in the DMN and FPN consistent with previous studies. In addition, we expected to elucidate new, less well-characterized regions showing an interaction between sex and aging, leading to a more complete picture of sex and aging effects on RSNs.

METHODS

Participants and Imaging Protocols

One hundred and three healthy right-handed adults, ages 18 to 65, participated in the study. Participants were recruited from the local area using posters and word of mouth, were screened using self-reports, and had no history of psychiatric or neurological illness. All participants

Abbreviations

BA	Brodmann area
CSF	Cerebral-spinal fluid
DMN	Default-mode network
fMRI	Functional magnetic resonance image
FPN	Fronto-parietal network
GSR	Global signal regression
ICA	Independent component analysis
ICD	Intrinsic connectivity distribution
LPFC	Lateral prefrontal cortex
MPFC	Medial prefrontal cortex
PCC	Posterior cingulate cortex
PPC	Posterior parietal cortex
RSN	Resting-state network

provided a written informed consent in accordance with a protocol approved by the Human Research Protection Program of Yale University. The analyses included 51 females (age = 33.3 ± 12.3) and 52 males (age = 34.9 ± 10.1).

Participants were scanned on two different Siemens 3T Tim Trio scanners at the Yale Magnetic Resonance Research Center and were instructed to rest with their eyes open, not to think of anything in particular, and not to fall asleep. The first 59 participants were scanned using a 12-channel head coil. The remaining 44 participants were scanned using a 32-channel head coil. There were no significant differences in the distribution of males and females or mean ages scanned between the two head coils ($P = 0.49$, $P = 0.07$) and between the two scanners ($P = 0.77$, $P = 0.38$). Supporting Information Table 1 provides a complete breakdown of age and sex for the different scanner configurations.

Each session began with a localizing scan, followed by a low-resolution sagittal scan for slice alignment, and the collection of 256-mm thick axial-oblique T1-weighted slices aligned with the AC-PC such that the top slice was at the top of the brain. Resting-state functional data was collected at the same slice locations as the T1-weighted anatomical data, using a T2*-sensitive gradient-recalled single shot echo-planar pulse sequence (TR = 1550 ms, TE = 30 ms, flip angle = 80 degrees, FOV = 220^2 mm, 64^2 matrix, resolution = 3.435 × 3.425 × 6 mm). There were eight functional runs, each containing 240 volumes (approximately 6 min, for a total of approximately 48 min continuous rest). The first six volumes of the functional runs were discarded to allow the signal to reach a steady-state. Finally, a high-resolution anatomical image was collected using an MPRAGE sequence (TR = 2530 ms, TE = 2.77 ms, TI = 1,100 ms, flip angle = 7 degrees, resolution = 1 mm^3).

Preprocessing

Images were slice-time corrected with sinc interpolation and motion corrected using SPM5 (http://www.fil.ion.ucl.ac.uk/spm/software/spm5/). All further analysis was performed using BioImage Suite (Joshi et al., 2011) unless otherwise specified. Several covariates of no interest were regressed from the data including linear and quadratic drift, six rigid-body motion parameters, mean cerebral-spinal fluid (CSF) signal, mean white-matter signal, and overall global signal. Next, the data were temporally smoothed with a zero-mean unit-variance Gaussian filter (approximate cutoff frequency=0.12Hz). Finally, a gray-matter mask was applied to the preprocessed data so that only voxels in the gray matter were used in the calculation. After preprocessing, all resting-state runs were concatenated for each participant and the connectivity for each voxel was then calculated in each participant's individual space.

Gray/white matter and CSF masks were defined on a template brain (Holmes et al., 1998), and warped to individual participant space using a series of transformations described below. The gray-matter mask was dilated to ensure full coverage of the gray matter after warping into individual participant space. Similarly, the white matter and CSF masks were eroded to ensure only pure white matter or CSF signal were regressed from the data.

Whole Brain Functional Connectivity

Functional connectivity of each voxel as measured by the ICD was calculated for each individual participant as described previously (Scheinost et al., 2012). ICD involves correlating the time course for each voxel with the time course of every other voxel in the brain and then summarizing these correlations with a network-theory metric. Specifically, ICD models the entire distribution of the network measure of degree, thereby eliminating the need to specify a connection threshold. Because the removal of the global mean makes the signs of the correlation ambiguous, we only focus on the positive correlation (Saad et al., 2012). A histogram of all positive correlations is constructed to estimate the distribution of connections to the current voxel. This distribution of connections is converted to a survival function, which is fitted with a stretched exponential with variance α. As the parameter α controls the spread of the distribution of connections, a larger α indicates a greater number of high correlation connections. Finally, this process is repeated for all voxels in the gray matter, resulting in a parametric image of the α parameter for each participant.

To interrogate relative differences in connectivity, each participant's map was normalized by subtracting the mean across all voxels and dividing by the standard deviation across all voxels. This z-score-like normalization does not change the underlying connectivity pattern but allows for investigation of relative differences in connectivity in the presence of large global differences in connectivity (Mitchell et al., 2013). This normalization also has been shown to reduce the impact of confounds related to motion (Yan et al., 2013).

Common Space Registration

To facilitate comparisons of imaging data, all single-participant ICD results were first spatially smoothed with a 6-mm Gaussian filter and warped to a common template space through the concatenation of a series of linear and non-linear registrations. The functional series were linearly registered to the T1 axial-oblique (2D anatomical) images. The 2D anatomical images were linearly registered to the MPRAGE (3D anatomical) images. The 3D anatomical images were non-linearly registered to the template brain. All transformation pairs were calculated independently and combined into a single transform warping the single-participant results into common space. This single transformation allows the single-participant images to be

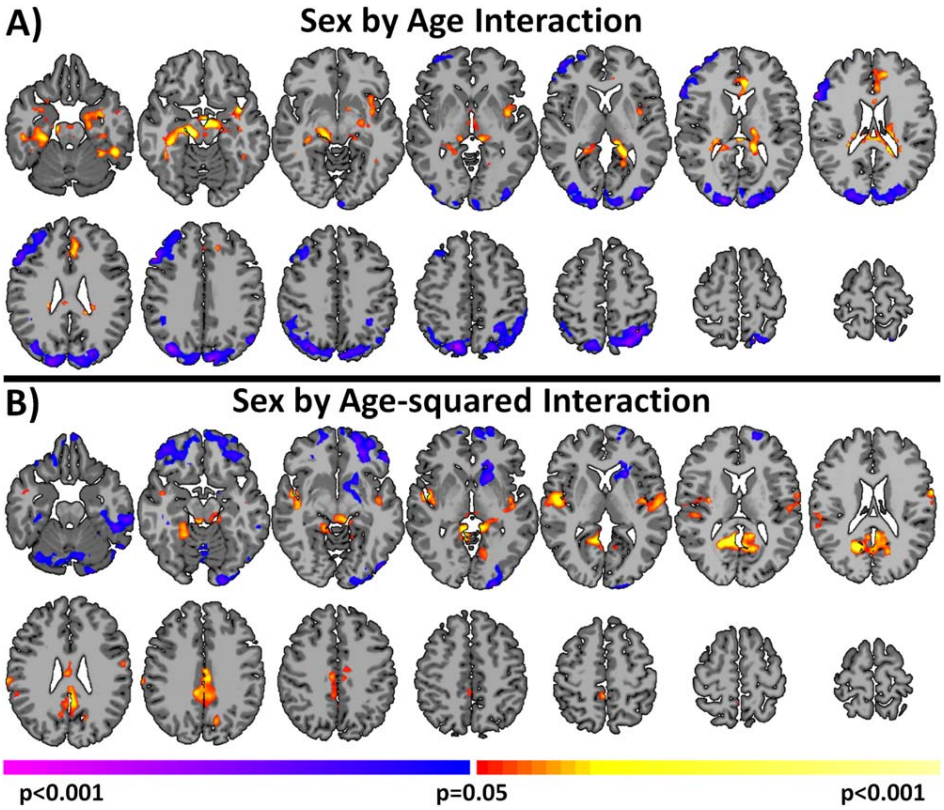

Figure 1.

Sex by aging interaction for connectivity. Sex by age interactions are shown in (**A**) and sex by age-squared interactions are shown in (**B**). Widespread significant ($P < 0.05$ corrected) differences in aging trajectories between males and females were observed. Warm colors represent areas where the slope associated with age or age-squared is greater for females compared to males. Cool colors represent areas where the slope associated with age or age-squared is greater for males compared to females. [Color figure can be viewed in the online issue, which is available at wileyonlinelibrary.com.]

transformed to common space with only one transformation, reducing interpolation error. All transformations were estimated using the intensity-based registration algorithms in BioImage Suite.

Group-Level Analyses

We examined changes in functional connectivity using general linear model (GLM) analyses aimed at detecting sex differences in aging. ICD results were modeled using sex, age, age-squared and their corresponding interactions (sex by age, and sex by age-squared) as independent variables of interest. Age was treated as a continuous variable. Several independent variables of no interest were included in the model to account for possible confounds. First, as gray-matter volume can differ between sexes (Gur et al., 1999), an estimate of each participant's gray-matter volume and its interaction with sex was included in the model. The gray-matter volume was estimated as the volume of the gray-matter mask used in the connectivity analysis. Second, as motion can confound many measures of functional connectivity (Van Dijk et al., 2012), the frame-to-frame displacement averaged across all functional volumes was include in the model. This approach has been shown to help minimize motion related confounds (Satterthwaite et al., 2012). Third, as three different scanner configurations were used to collect the data (a 16- or 32-channel head coil on the first scanner, or 32-channel head coil on the second scanner), scanner and head coil were included in the model. The full model used to examine sex differences in aging was:

$$\begin{aligned}\mathrm{ICD}_{i,j} = {} & \beta_{0,j} + \beta_{1,j} \times \mathrm{sex}_i + \beta_{2,j} \times \mathrm{age}_i + \beta_{3,j} \times \mathrm{age}^2{}_i + \beta_{4,j} \times \mathrm{sex}_i \\ & \times \mathrm{age}_i + \beta_{5,j} \times \mathrm{sex}_i \times \mathrm{age}^2{}_i + \beta_{6,j} \times \mathrm{GM\ volume}_i + \beta_{7,j} \\ & \times \mathrm{sex}_i \times \mathrm{GM\ volume}_i + \beta_{8,j} \times \mathrm{motion}_i + \beta_{9,j} \times \mathrm{scanner}_i \\ & + \beta_{10,j} \times \mathrm{head\ coil}_i + \varepsilon_{i,j},\end{aligned}$$

The subscript i indexes the participant and the subscript j indexes the spatial location (voxel). The error term is

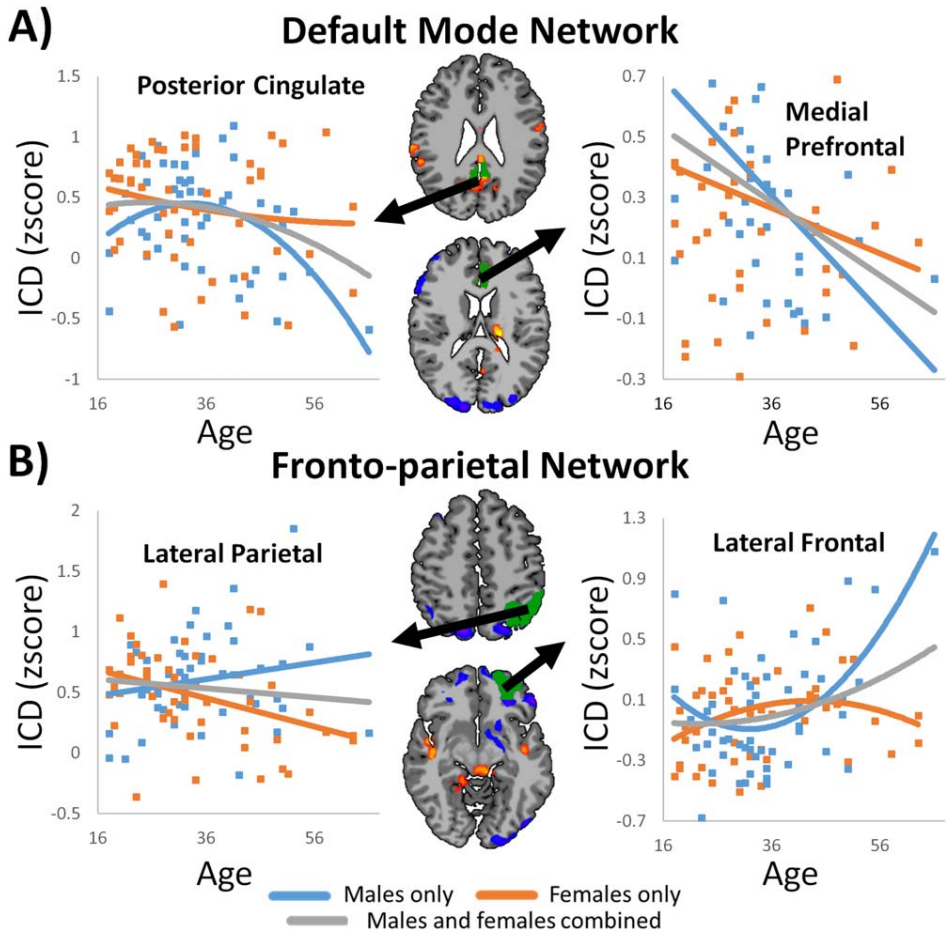

Figure 2.

Scatterplots for sex by aging interaction in (**A**) DMN and (**B**) FPN. (A) For both DMN nodes, males displayed a greater change in connectivity per yearly increase in age compared to females. (B) For both FPN nodes, males and females showed divergent directions of aging trajectories with males showing increased connectivity with age and females showing decreased connectivity with age. [Color figure can be viewed in the online issue, which is available at wileyonlinelibrary.com.]

denote as ε_{ij}. The model parameters were estimated using AFNI's 3dLME (Chen et al., 2013).

Significance was assessed at a $P < 0.05$ level after correcting for multiple comparisons across the gray matter via AFNI's AlphaSim program. All results were also localized in terms of the Brodmann areas (BA) identified using BioImage Suite's digital Brodmann atlas.

RESULTS

The Results section is organized as follows. First, we present results demonstrating significant sex by aging interactions. Next, we present main effects of sex and aging, respectively, focusing mainly on regions that show these main effects but not significant sex by aging interaction. Finally, we compare results with and without global signal regression (GSR), highlighting the robustness of our results to this preprocessing choice.

Interaction Between Sex and Aging

Widespread significant ($P < 0.05$ corrected) sex by aging (either age or age-squared) interactions were observed in many large-scale RSNs as shown in Figure 1. These RSNs include the DMN, the FPN, the visual network, the auditory network, and several subcortical networks. A full list of brain regions displaying a significant sex by age or sex by age-squared interaction ($P < 0.05$, corrected) is

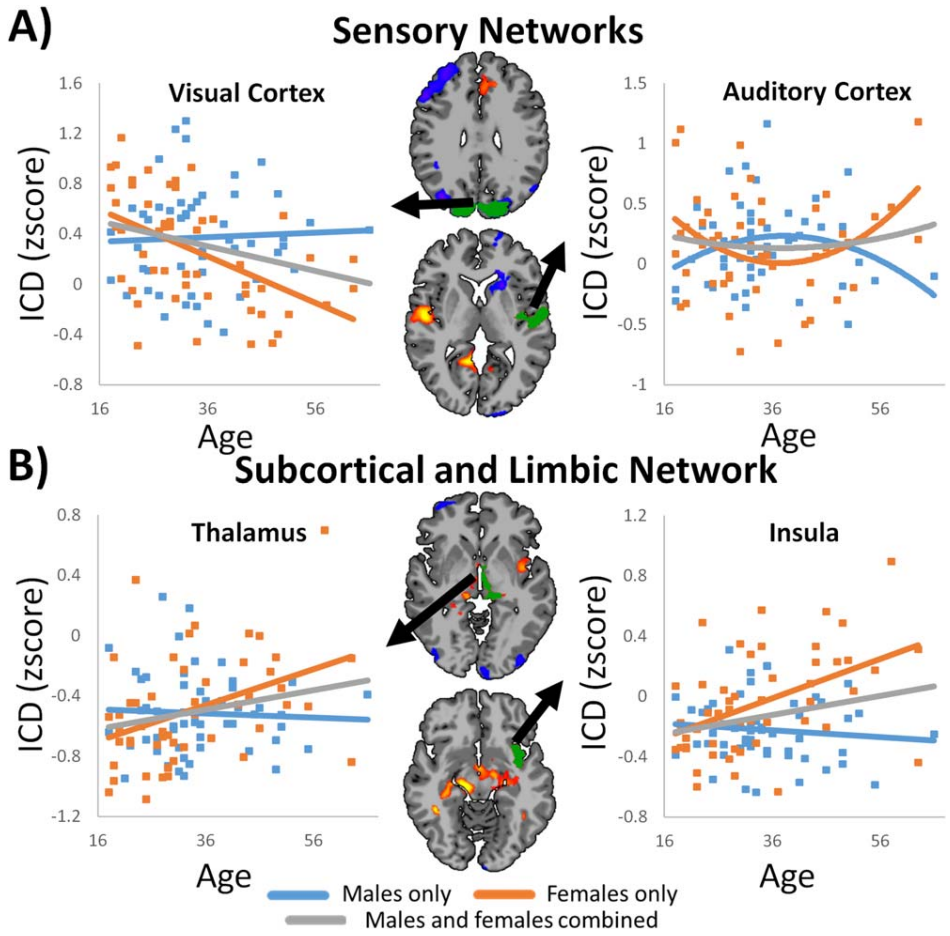

Figure 3.

Scatterplots for sex by aging interaction in (**A**) sensory and (**B**) subcortical and limbic networks. (A) Sensory networks displayed sex by aging interaction in the visual and auditory networks. (B) Females showed increased connectivity with age in many subcortical and limbic regions, whereas males showed little change in connectivity with age. [Color figure can be viewed in the online issue, which is available at wileyonlinelibrary.com.]

presented in Supporting Information Table SII and Table SIII, respectively.

The posterior cingulate cortex (PCC) and the medial prefrontal cortex (MPFC), both key nodes of the DMN, displayed a prominent sex by aging interaction (see Fig. 1A,B, respectively). As shown in Figure 2A, both sexes showed a decrease in connectivity with age in the PCC. Males showed a non-linear change in connectivity, with older participants displaying a sharper decrease in connectivity than younger participants, whereas females showed a more linear decrease in connectivity with age. Similarly, in the MPFC, males displayed a steeper slope between age and connectivity compared to females (Fig. 2A).

Both the lateral prefrontal cortex (LPFC) and the posterior parietal cortex (PPC) regions of the FPN displayed significant sex by aging interactions (Fig. 1A). For these regions, males displayed a positive correlation with age or age-squared; while, females demonstrated either no correlation or a slight inverse correlation with age or age-squared. Examples of this interaction are shown in Figure 2B for the left PPC and left inferior LPFC. The right LPFC and right PPC (not shown) show similar patterns.

Basic sensory networks also showed significant interaction between sex and aging. Females displayed an inverse correlation with age in primary visual cortex. In contrast, males displayed little or no correlation with age (Fig. 3A). In the right and left auditory cortex, a sex by age-squared interaction was observed (Figs. 1B and 3A). Males demonstrated an increase in connectivity with peak connectivity in the mid 30's, and a decrease in connectivity afterwards. Females demonstrated the opposite trend, showing the lowest connectivity in the mid 30's and peaking at early adulthood and late middle age (Fig. 3A).

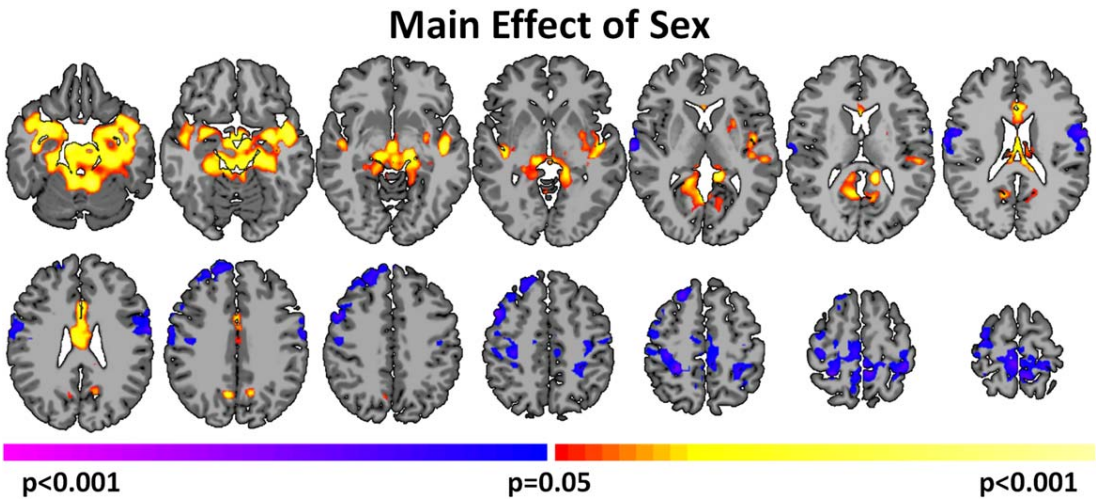

Figure 4.

Sex Differences in connectivity. Widespread significant ($P < 0.05$ corrected) differences between males and females were observed. Warm colors represent areas with greater connectivity for females compared with males. Cool colors represent areas with greater connectivity for males compared with females. [Color figure can be viewed in the online issue, which is available at wileyonlinelibrary.com.]

Finally, many subcortical and limbic regions displayed a sex by aging interaction. A sex by age interaction was observed in bilateral parahippocampal gyrus, bilateral hippocampus, left insular cortex, left thalamus, and left amygdala (Fig. 1A). As shown in Figure 3B, females tended to exhibit strong positive correlation with age; while, males tended to exhibit little or no correlation with age. A sex by age-squared interaction was observed in the left caudate (Fig. 1B).

Main Effect of Sex

The ICD analysis for this group of participants revealed sex-related differences in connectivity throughout the brain as shown in Figure 4. Significant increased connectivity for males compared to females that did not overlap with regions showing significant interactions was observed in the sensorimotor network, including bilateral primary motor, primary sensory, and premotor cortices, as well as the supplementary motor area and superior right amygdala. Significant increased connectivity for females compared to males was observed in subcortical and limbic areas. Most of these regions displaying significant sex differences also showed a significant sex by aging (either age or age^2) interaction. A full list of brain regions displaying significant sex by aging interaction ($P < 0.05$ corrected) is presented in Supporting Information Table SIV.

Main Effect of Aging

Linear and non-linear (quadratic) maturations of global connectivity are shown in Figure 5. Similar to the main effect of sex, many of these regions displayed a significant sex by aging (either age or age-squared) interaction. Significant positive correlations with age (absent of a significant sex by aging interaction) were observed in the bilateral putamen, right caudate, right amygdala, and the orbital frontal cortex. While a significant sex by age interaction was observed in the left thalamus, the main effect of age observed in the thalamus was bilateral and more prominent. Significant inverse correlations with age were observed in the inferior occipital lobe. These regions included BA 19, a portion of the fusiform cortex, and visual association cortices. Additionally, the lateral parietal portion of the DMN was inversely correlated with age. The right inferior frontal gyrus displayed a significant correlation with age-squared, but did not display a significant sex by aging interaction. A full list of brain regions displaying significant correlation with either age or age-squared ($P < 0.05$ corrected) is presented in Supporting Information Table SV and SVI, respectively.

Robustness of Results to Global Signal Regression

Global signal regression (GSR; performed in this work) remains a controversial preprocessing step as GSR changes the correlation structure between brain regions (Saad et al., 2012) and may distort group comparisons (Gotts et al., 2013). To highlight the robustness of our results with respect to preprocessing choice, we repeated all analyses without removing the global signal. As shown in Figure 6, the results with and without GSR are largely the same.

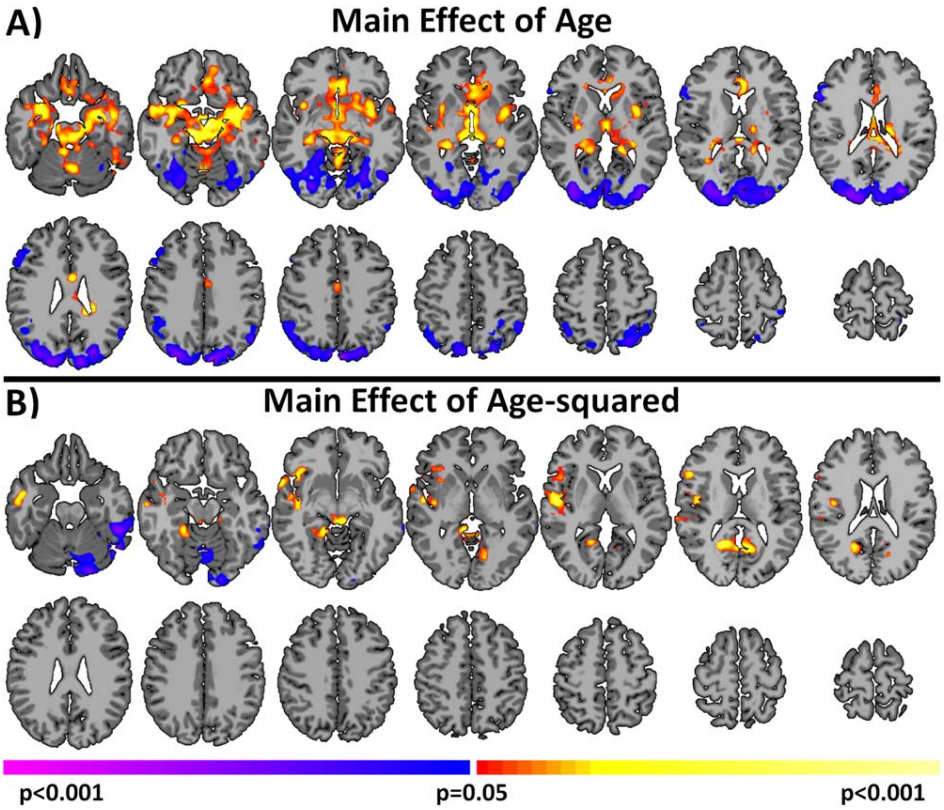

Figure 5.

Linear and non-linear effects of aging on connectivity. Widespread significant ($P < 0.05$ corrected) correlations with age and age-squared were observed. (**A**) Correlations with age. (**B**) Correlations with age-squared. These maps are collapsed across males and females. Warm colors represent areas with a positive correlation with age or age-squared. Cool colors represent areas with negative correlations with age or age-squared. [Color figure can be viewed in the online issue, which is available at wileyonlinelibrary.com.]

DISCUSSION

Using a voxel-wise measure of functional brain organization and general linear modeling, these data demonstrate that males and females show differential patterns of changing connectivity in large-scale RSNs during normal aging from early adulthood to late middle-age. In some networks, such as the DMN, males and females both showed age-related decreases in connectivity, albeit at different rates. In other networks, such as the FPN, males and females showed divergent aging trajectories. Main effects of sex and aging were found in many of the same regions showing sex-related differences in aging. Finally, these sex differences in aging trajectories were robust to choice of preprocessing strategy.

Our results highlight the influence of sex on age-related changes in connectivity, especially in the DMN. Changes in DMN connectivity due to age are well-characterized, with studies generally reporting a decrease in DMN connectivity with age (Allen et al., 2011; Andrews-Hanna et al., 2007; Biswal et al., 2010; Damoiseaux et al., 2008; Hampson et al., 2012) and a greater rate of change in older participants compared to younger participants (Andrews-Hanna et al., 2007). Our results are largely in agreement, and, at the same time, extend these previous findings by suggesting that males have a greater rate of decrease in DMN connectivity with age than females. As shown in Figure 2A, a non-linearly decreasing relationship between age and connectivity in PCC was observed in males, but not females. Likewise, in regions where both males and females displayed a linear decrease in connectivity with age (such as the MPFC; Fig. 2A), males exhibited a significantly steeper slope. As decreased connectivity in regions of the DMN are potentially important markers for disorders such as Alzheimer's disease (Chhatwal et al., 2013; Damoiseaux, 2012), accurate mapping of sex-related differences in aging may eventually help distinguish normal aging from clinical pathology.

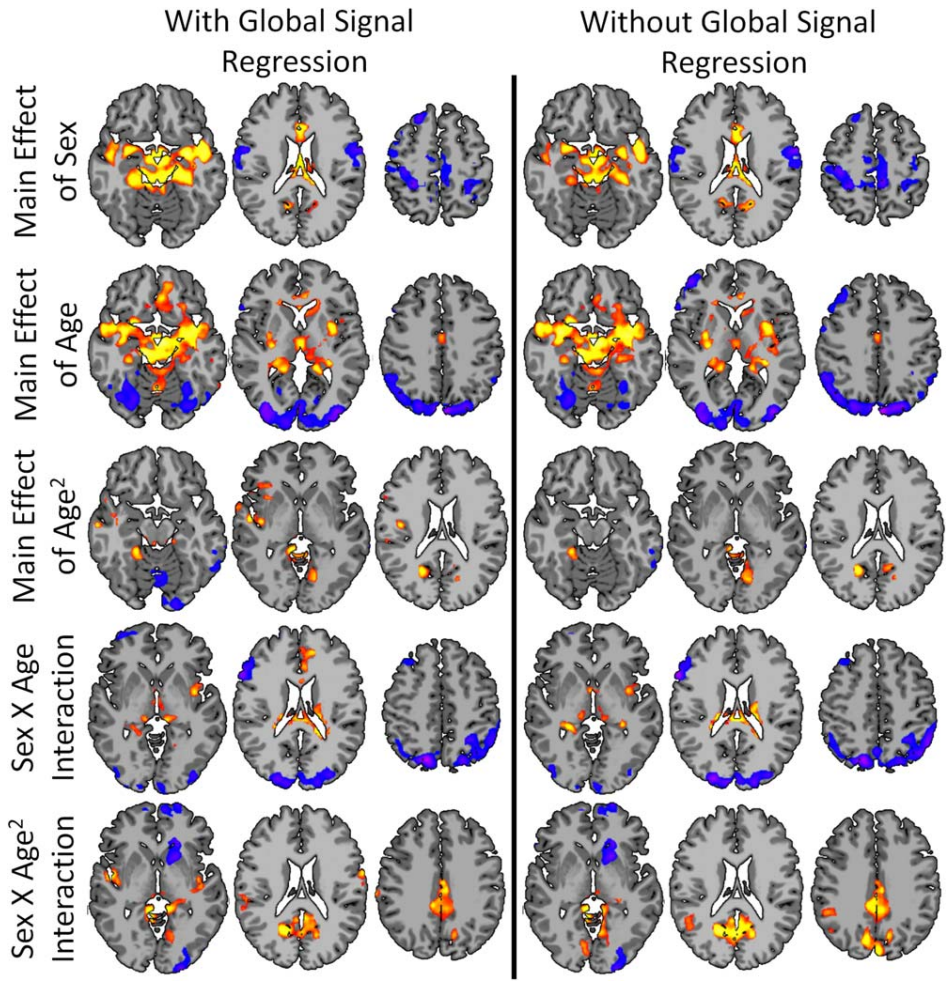

Figure 6.

Robustness of results to preprocessing. The observe sex differences in aging trajectories were robust to choice of preprocessing strategy. The results with (right column) and without GSR (left column) are largely the same. [Color figure can be viewed in the online issue, which is available at wileyonlinelibrary.com.]

Reports of sex differences in the DMN have been inconsistent across studies. Several studies report either no or minor differences in DMN connectivity (Bluhm et al., 2008; Weissman-Fogel et al., 2010). In contrast, studies using larger, multi-site samples report greater connectivity in the DMN for females compared to males (Allen et al., 2011; Biswal et al., 2010; Tomasi and Volkow, 2012b). Importantly, regions of greater DMN (i.e., PCC, and MPFC) connectivity for females compared to males overlapped with regions of greater DMN connectivity for younger participants compared to older participants (Biswal et al., 2010). These disagreements in the literature may be explained by the observed interactions between sex and aging in DMN connectivity (Figs. 1 and 2A). For example, studies with younger participants may not show significant sex effects. However, if older participants are included in the sample, significant sex effects could be observed even with age-matched participants, as our results suggest that males "age" more quickly in many regions of the DMN.

In contrast to the DMN, which showed decreasing connectivity with age for both males and females, the FPN showed divergent aging trajectories for males and females. When the groups were combined, an overall negative correlation with age was observed consistent with previous reports (Allen et al., 2011; Geerligs et al., in press; Tomasi and Volkow, 2012a). Yet, with a more holistic analysis allowing for sex-specific aging, this negative correlation with age was only found in females. Sex by age interactions have also been reported in similar regions of the FPN in the LPFC using other connectivity methods (Zuo et al., 2010).

Aging trajectories of connectivity in the DMN and the FPN have been associated with cognitive performance. In the context of age differences, lower performance on cognitive measures has been linked to lower connectivity in the DMN (Damoiseaux et al., 2008; Geerligs et al., in press) and the FPN (Geerligs et al., in press; Grady et al., 2010). Greater plasticity of the FPN has been linked to higher cognitive performance (Cole et al., 2013; Grady et al., 2010), and may be a compensatory mechanism for age reductions in DMN connectivity (Grady et al., 2010). Our results provide further evidence for this interplay of DMN and FPN connectivity profiles across age. Males displayed steeper changes in DMN connectivity, especially in the PCC, but showed smaller changes (and possible increases) in connectivity for the lateral prefrontal regions of the FPN. Conversely, females displayed milder changes in DMN connectivity, but showed larger decreases in FPN connectivity. Overall, age-related changes in DMN connectivity, FPN connectivity, and cognitive functions could have an interdependent relationship moderated by sex.

Many subcortical and limbic regions displayed widespread effects of sex and aging, in addition to sex by aging interactions. In these regions (such as the parahippocampal gyrus, hippocampus, insula, thalamus, and amygdala), older females displayed the greatest connectivity, while younger females, younger males and older males displayed similar levels of connectivity (see Fig. 3B). As many of these regions play a role in affective functions (Davidson and Irwin, 1999), this increased connectivity in older females may be related to changes in emotion processing. Likewise, studies of emotional control have shown improved control with aging in females but not males (Gross et al., 1997). The increase in connectivity for older females is largely responsible for the observed main effects that females have greater connectivity than males (Fig. 4) and that connectivity increases with age (Fig. 5).

In addition to the networks responsible for higher-order executive functions, networks responsible for the basic senses showed differential aging patterns for males and females. An inverse correlation between connectivity and aging in the visual network was observed for females, but not males. Lesser connectivity for females in the visual network has been found previously (Filippi et al., 2013). These differences in visual network connectivity reported in the literature may be related to our observed interaction effects, as older females may reduce the overall mean female connectivity in the visual network, leading to a group difference. Primary motor cortex showed greater connectivity in males when compared to females. Some studies report that males demonstrate better motor and spatial abilities (Gur et al., 2012; Jones et al., 2003), which may be related to the observed connectivity differences in the sensorimotor network.

Strengths of this study include large amount of rs-fMRI data per participant, linear modeling of sex-specific aging trajectories, and employment of a threshold-free graph theory measure. In contrast to many studies where only 5–15 minutes of rs-fMRI data is available, this study consisted of nearly 50 minutes of data per participant which can minimize the variance associated voxelwise correlations. Modeling sex by aging interactions allows for a more complete characterization of sex and aging effects and reveals new sex-specific aging trajectories. ICD is a novel voxelwise measure that does not rely on thresholds in assessing connectivity. Many previous studies of sex differences have relied on ICA (Allen et al., 2011; Biswal et al., 2010; Bluhm et al., 2008; Filippi et al., 2013; Weissman-Fogel et al., 2010). Discrepancies between these earlier studies and the results presented here likely reflect the methodological differences, and possibly improved sensitivity gained by using large amounts of rs-fMRI data and a voxelwise connectivity measure.

Limitations of this study include the lack of behavioral measures to correlate with aging, a restricted age range, and the cross-sectional rather than longitudinal nature of the study. Without behavioral correlates, the observed changes in connectivity cannot be directly related to changes in cognitive function. The age range of our sample only included one participant older than 65, providing limited conclusions about aging in older adults. A cross-sectional design affords snapshots of individuals that are pieced together to infer trends of aging over the larger population (Karmiloff-Smith, 2010). However, individuals may age at different rates throughout the lifespan, and thus longitudinal imaging and paired connectivity methods (Scheinost et al., 2014) could greatly improve the estimation of rs-fMRI characteristics of sex and aging.

In conclusion, men and women show differential patterns of changing connectivity with age across the lifespan. These sex differences in aging may play a role in age-related changes in normal cognition, as well as susceptibility to neurological/psychiatric diseases and disorders. Further work is needed to understand how these differences relate to personality, behavioral traits, and disease and how they are influenced by different social/environmental contexts. Finally, these results replicate many previous findings and also reveal new insights on how sex and age moderate functional connectivity in the brain, arguing for careful consideration of these basic demographic variables in rs-fMRI studies.

REFERENCES

Allen EA, Erhardt EB, Damaraju E, Gruner W, Segall JM, Silva RF, Havlicek M, Rachakonda S, Fries J, Kalyanam R, Michael AM, Caprihan, A, Turner JA, Eichele T, Adelsheim S, Bryan AD, Bustillo J, Clark VP, Feldstein Ewing SW, Filbey F, Ford CC, Hutchison K, Jung RE, Kiehl KA, Kodituwakku P, Komesu YM, Mayer AR, Pearlson GD, Phillips JP, Sadek JR, Stevens M, Teuscher U, Thoma RJ, Calhoun VD (2011): A baseline for the multivariate comparison of resting-state networks. Front Syst Neurosci 5:2.

Andrews-Hanna JR, Snyder AZ, Vincent JL, Lustig C, Head D, Raichle ME, Buckner RL (2007): Disruption of large-scale brain systems in advanced aging. Neuron 56:924–935.

Biswal BB, Mennes M, Zuo XN, Gohel S, Kelly C, Smith SM, Beckmann CF, Adelstein JS, Buckner RL, Colcombe S, Dogonowski AM, Ernst M, Fair D, Hampson M, Hoptman MJ, Hyde JS, Kiviniemi VJ, Kötter R, Li SJ, Lin CP, Lowe MJ, Mackay C, Madden DJ, Madsen KH, Margulies DS, Mayberg HS, McMahon K, Monk CS, Mostofsky SH, Nagel BJ, Pekar JJ, Peltier SJ, Petersen SE, Riedl V, Rombouts SA, Rypma B, Schlaggar BL, Schmidt S, Seidler RD, Siegle GJ, Sorg C, Teng GJ, Veijola J, Villringer A, Walter M, Wang L, Weng XC, Whitfield-Gabrieli S, Williamson P, Windischberger C, Zang YF, Zhang H.Y, Castellanos FX, Milham MP (2010): Toward discovery science of human brain function. Proc Natl Acad Sci U S A 107:4734–4739.

Bluhm RL, Osuch EA, Lanius RA, Boksman K, Neufeld RW, Théberge J, Williamson P (2008): Default mode network connectivity: Effects of age, sex, and analytic approach. Neuroreport 19:887–891.

Buckner RL, Andrews-Hanna JR, Schacter DL (2008): The brain's default network: Anatomy, function, and relevance to disease. Ann N Y Acad Sci 1124:1–38.

Chen G, Saad ZS, Britton JC, Pine DS, Cox RW (2013): Linear mixed-effects modeling approach to FMRI group analysis. Neuroimage 73:176–190.

Chhatwal JP, Schultz AP, Johnson K, Benzinger TL, Jack C, Ances BM, Sullivan CA, Salloway SP, Ringman JM, Koeppe RA, Marcus DS, Thompson P, Saykin AJ, Correia S, Schofield PR, Rowe CC, Fox NC, Brickman AM, Mayeux R, McDade E, Bateman R, Fagan AM, Goate AM, Xiong C, Buckles VD, Morris JC, Sperling RA (2013): Impaired default network functional connectivity in autosomal dominant Alzheimer disease. Neurology 81:736–744.

Cole MW, Yarkoni T, Repovs G, Anticevic A, Braver TS (2012): Global connectivity of prefrontal cortex predicts cognitive control and intelligence. J Neurosci 32:8988–8999.

Cole MW, Reynolds JR, Power JD, Repovs G, Anticevic A, Braver TS (2013): Multi-task connectivity reveals flexible hubs for adaptive task control. Nat Neurosci 16:1348–1355.

Cosgrove KP, Mazure CM, Staley JK (2007): Evolving knowledge of sex differences in brain structure, function, and chemistry. Biol Psychiatry 62:847–855.

Damoiseaux JS (2012): Resting-state fMRI as a biomarker for Alzheimer's disease? Alzheimers Res Ther 4:8.

Damoiseaux JS, Rombouts SA, Barkhof F, Scheltens P, Stam CJ, Smith SM, Beckmann CF (2006): Consistent resting-state networks across healthy subjects. Proc Natl Acad Sci U S A 103: 13848–13853.

Damoiseaux JS, Beckmann CF, Arigita EJ, Barkhof F, Scheltens P, Stam CJ, Smith SM, Rombouts SA (2008): Reduced resting–state brain activity in the "default network" in normal aging. Cereb Cortex 18:1856–1864.

Davidson RJ, Irwin W (1999): The functional neuroanatomy of emotion and affective style. Trends Cogn Sci 3:11–21.

Fair DA, Cohen AL, Power JD, Dosenbach NU, Church JA, Miezin FM, Schlaggar BL, Petersen SE (2009): Functional brain networks develop from a "local to distributed" organization. PLoS Comput Biol 5:e1000381.

Filippi M, Valsasina P, Misci P, Falini A, Comi G, Rocca MA (2013): The organization of intrinsic brain activity differs between genders: A resting-state fMRI study in a large cohort of young healthy subjects. Hum Brain Mapp 34:1330–1343.

Geerligs L, Renken RJ, Saliasi E, Maurits NM, Lorist MM: A brain-wide study of age-related changes in functional connectivity. Cereb Cortex. 2014 Feb 13. [Epub ahead of print]

Gotts SJ, Saad ZS, Jo HJ, Wallace GL, Cox RW, Martin A (2013): The perils of global signal regression for group comparisons: A case study of Autism Spectrum Disorders. Front Hum Neurosci 7:356.

Grady CL, Protzner AB, Kovacevic N, Strother SC, Afshin-Pour B, Wojtowicz M, Anderson JA, Churchill N, McIntosh AR (2010): A multivariate analysis of age-related differences in default mode and task-positive networks across multiple cognitive domains. Cereb Cortex 20:1432–1447.

Gross JJ, Carstensen LL, Pasupathi M, Tsai J, Skorpen CG, Hsu AY (1997): Emotion and aging: Experience, expression, and control. Psychol Aging 12:590–599.

Gur RC, Turetsky BI, Matsui M, Yan M, Bilker W, Hughett P, Gur RE (1999): Sex differences in brain gray and white matter in healthy young adults: Correlations with cognitive performance. J Neurosci 19:4065–4072.

Gur RC, Richard J, Calkins ME, Chiavacci R, Hansen JA, Bilker WB, Loughead J, Connolly JJ, Qiu H, Mentch FD, Abou-Sleiman PM, Hakonarson H, Gur RE (2012): Age group and sex differences in performance on a computerized neurocognitive battery in children age 8–21. Neuropsychology 26:251–265.

Hampson M, Tokoglu F, Sun Z, Schafer RJ, Skudlarski P, Gore JC, Constable RT (2006): Connectivity-behavior analysis reveals that functional connectivity between left BA39 and Broca's area varies with reading ability. NeuroImage 31:513–519.

Hampson M, Tokoglu F, Shen X, Scheinost D, Papademetris X, Constable RT (2012): Intrinsic brain connectivity related to age in young and middle aged adults. PLoS One 7:e44067.

Holmes CJ, Hoge R, Collins L, Woods R, Toga AW, Evans AC (1998): Enhancement of MR images using registration for signal averaging. J Comp Assist Tomography 22:324–333.

Jones CM, Braithwaite VA, Healy SD (2003): The evolution of sex differences in spatial ability. Behav Neurosci 117:403–411.

Joshi A, Scheinost D, Okuda H, Belhachemi D, Murphy I, Staib LH, Papademetris X (2011): Unified framework for development, deployment and robust testing of neuroimaging algorithms. Neuroinformatics 9:69–84.

Karmiloff-Smith A (2010): Neuroimaging of the developing brain: Taking "developing" seriously. Hum Brain Mapp 31:934–941.

Mitchell MR, Balodis IM, Devito EE, Lacadie CM, Yeston J, Scheinost D, Constable RT, Carroll KM, Potenza MN (2013): A preliminary investigation of Stroop-related intrinsic connectivity in cocaine dependence: Associations with treatment outcomes. Am J Drug Alcohol Abuse 39:392–402.

Saad ZS, Gotts SJ, Murphy K, Chen G, Jo HJ, Martin A, Cox RW (2012): Trouble at rest: How correlation patterns and group differences become distorted after global signal regression. Brain Connect 2:25–32.

Satterthwaite TD, Wolf DH, Loughead J, Ruparel K, Elliott MA, Hakonarson H, Gur RC, Gur RE (2012): Impact of in-scanner head motion on multiple measures of functional connectivity: Relevance for studies of neurodevelopment in youth. Neuroimage 60:623–632.

Scheinost D, Benjamin J, Lacadie CM, Vohr B, Schneider KC, Ment LR, Papademetris X, Constable RT (2012): The intrinsic connectivity distribution: A novel contrast measure reflecting voxel level functional connectivity. NeuroImage, 62:1510–1519.

Scheinost D, Shen X, Finn E, Sinha R, Constable RT, Papademetris X (2014): Coupled intrinsic connectivity distribution analysis: A method for exploratory connectivity analysis of paired FMRI data. PLoS One 9:e93544.

Smith SM, Fox PT, Miller KL, Glahn DC, Fox PM, Mackay CE, Filippini N, Watkins KE, Toro R, Laird AR, Beckmann CF (2009): Correspondence of the brain's functional architecture during activation and rest. Proc Natl Acad Sci U S A 106: 13040–13045.

Svensén M, Kruggel F, Benali H (2002): ICA of fMRI group study data. Neuroimage 16:551–563.

Tomasi D, Volkow ND (2012a): Aging and functional brain networks. Mol Psychiatry 17:471, 549–558.

Tomasi D, Volkow ND (2012b): Gender differences in brain functional connectivity density. Hum Brain Mapp 33:849–860.

Van Dijk KR, Sabuncu MR, Buckner RL (2012): The influence of head motion on intrinsic functional connectivity MRI. Neuroimage 59:431–438.

Weissman-Fogel I, Moayedi M, Taylor KS, Pope G, Davis KD (2010): Cognitive and default-mode resting state networks: Do male and female brains "rest" differently? Hum Brain Mapp 31:1713–1726.

Yan CG, Cheung B, Kelly C, Colcombe S, Craddock RC, Di Martino A, Li Q, Zuo XN, Castellanos FX, Milham MP (2013): A comprehensive assessment of regional variation in the impact of head micromovements on functional connectomics. Neuroimage 76:183–201.

Yeo BT, Krienen FM, Sepulcre J, Sabuncu MR, Lashkari D, Hollinshead M, Roffman JL, Smoller JW, Zöllei L, Polimeni JR, Fischl B, Liu H, Buckner RL (2011): The organization of the human cerebral cortex estimated by intrinsic functional connectivity. J Neurophysiol 106:1125–1165.

Zuo XN, Kelly C, Di Martino A, Mennes M, Margulies DS, Bangaru S, Grzadzinski R, Evans AC, Zang YF, Castellanos FX, Milham MP (2010): Growing together and growing apart: Regional and sex differences in the lifespan developmental trajectories of functional homotopy. J Neurosci 30: 15034–15043.